Stochastic Hydrology and Hydraulics 11: 193-210 © Springer-Verlag 1997

An analysis of the characteristics of rough bed turbulent shear stresses in an open channel

A. Keshavarzy and **J. E. Ball**
Water Research Lab, University of New South Wales, King Street, Manly Vale 2093, Australia

Abstract: Entrainment of sediment particles from channel beds into the channel flow is influenced by the characteristics of the flow turbulence which produces stochastic shear stress fluctuations at the bed. Recent studies of the structure of turbulent flow has recognized the importance of bursting processes as important mechanisms for the transfer of momentum into the laminar boundary layer. Of these processes, the sweep event has been recognized as the most important bursting event for entrainment of sediment particles as it imposes forces in the direction of the flow resulting in movement of particles by rolling, sliding and occasionally saltating. Similarly, the ejection event has been recognized as important for sediment transport since these events maintain the sediment particles in suspension.

In this study, the characteristics of bursting processes and, in particular, the sweep event were investigated in a flume with a rough bed. The instantaneous velocity fluctuations of the flow were measured in two-dimensions using a small electromagnetic velocity meter and the turbulent shear stresses were determined from these velocity fluctuations. It was found that the shear stress applied to the sediment particles on the bed resulting from sweep events depends on the magnitude of the turbulent shear stress and its probability distribution. A statistical analysis of the experimental data was undertaken and it was found necessary to apply a Box-Cox transformation to transform the data into a normally distributed sample. This enabled determination of the mean shear stress, angle of action and standard error of estimate for sweep and ejection events. These instantaneous shear stresses were found to be greater than the mean flow shear stress and for the sweep event to be approximately 40 percent greater near the channel bed.

Results from this analysis suggest that the critical shear stress determined from Shield's diagram is not sufficient to predict the initiation of motion due to its use of the temporal mean shear stress. It is suggested that initiation of particle motion, but not continuous motion, can occur earlier than suggested by Shield's diagram due to the higher shear stresses imposed on the particles by the stochastic shear stresses resulting from turbulence within the flow.

Key words: Turbulence, sediment, fluvial, river, bursting process, statistics.

1 Introduction

The motion of sediment particles and the initiation of that motion is an important component of many engineering studies. For example, there is a need to quantify the threshold conditions for entrainment of sediment particles in the design of stable

channels, bank protection works, and, in general, problems associated with the erosion of channels. Further problems where the initiation of sediment particle motion is imp arise when motion of pollutants attached to sediment particles becomes an important component of managing water quality.

There are many processes which influence the availability and entrainment of sediment particles; among these influences, the flow turbulence and the associated coherent structures within the flow are very important but, as yet, have not been defined completely. In this regard, Nezu and Nakagawa (1993) pointed out that the mechanism of turbulence production in flow over rough beds in rivers required investigation. Associated with this production of turbulence and the resultant momentum transfer are the processes by which constituents such as sediment particles are entrained and moved with the flow.

Recent research has focused on developing an understanding of the processes influencing and the mechanisms related to the transfer of momentum between the laminar and turbulent regions of the boundary layer. Several alternative models have been developed for the description of turbulent flow within and near the boundary layer', see, for example, Grass (1971), Offen and Kline (1975), and Raupach (1981) for a description of some of these models. In general, these models considered the mean velocity profile within the flow and the statistical characteristics of the coherent turbulent structures within the flow.

The concept of the bursting phenomenon was introduced by Kline et al. (1967) as a means of describing the transfer of momentum between the turbulent and laminar regions near the boundary. Four (4) quadrants or classes of events were identified. Each event was classified according to the quadrant associated with the velocity fluctuations occurring during the event. These velocity fluctuations (u',v') are defined as the variations from the temporal mean velocities in the longitudinal and vertical directions. Algebraically, they are defined by

$$u' = u - \overline{u} \tag{1}$$

and

$$v' = v - \overline{v} \tag{2}$$

where u and v are the instantaneous velocities in the longitudinal and vertical directions respectively and $\overline{u}$ and $\overline{v}$ are the temporal mean velocities in the longitudinal and vertical directions. These temporal mean velocities are given by

$$\overline{u} = \frac{1}{N} \sum_{i=1}^{n} u_i \tag{3}$$

and

$$\overline{v} = \frac{1}{N} \sum_{i=1}^{n} v_i \tag{4}$$

where N is the number of instantaneous velocity samples.

The four quadrants identified for the velocity fluctuations and the associated bursting event were

- outward interaction or quadrant I (upward front), in which $u' > 0$ and $v' > 0$;
- ejection event or quadrant II (upward back), in which $u' < 0$ and $v' > 0$;
- inward interaction or quadrant III (downward back), in which $u' < 0$ and $v' < 0$; and
- sweep event or quadrant IV (downward front), in which $u' > 0$ and $v' < 0$.

Shown in Figure 1 is a phase diagram with the quadrant of each event class indicated. It is obvious from this figure that sweep events result in a velocity vector angled towards the bed. Therefore, bursting events in this quadrant will have a significant influence on the entrainment of particles into the flowing water. Of particular is the magnitude of the horizontal velocity component during quadrant IV events and the angle which the velocity vector impacts on the bed particles.

In recent years, the contributions of coherent structures, such as the sweep (quadrant IV) and ejection (quadrant II events, to momentum transfer have been extensively studied by quadrant analysis or probability analyses based on two-dimensional velocity information. Studies by Nakagawa and Nezu (1978) and Grass (1971, 1982) have indicated that just above the channel bed, the sweep event is more responsible than the ejection event for transfer of momentum into the boundary layer. In addition, Nakagawa and Nezu (1978), Thorne et al. (1989), and Keshavarzy and Ball (1995) pointed out that the sweep and ejection events occur more frequently than the outward interaction (quadrant I) and inward interaction (quadrant III) events.

The four types of bursting events identified earlier have different influences on the rate, and mechanisms of sediment entrainment in a turbulent flow. In studies of sediment transport by, for example, Williams (1990) and Thorne et al. (1989), it has been shown that sediment entrainment occurs from the bed most frequently during sweep events and only occasionally during outward interaction events, whereas transport of suspended sediment depends primarily on the ejection event. Additionally, Keshavarzy and Ball (1995) pointed out that the magnitude of the instantaneous shear stress in a sweep event is greater than that which occurs during both outward and inward interaction events. These bursting events impose a rapid and significant pressure fluctuation on the bed; it is these fluctuations that are considered to have a significant influence on the entrainment of sediment particles from the bed with a resultant temporally variable sediment transport rate. These instantaneous pressure fluctuations lower the local pressure near the bed and hence particles may be ejected from the bed by hydrostatic pressure. Raudkivi (1990) postulated that even sheltered particles can be entrained by this mechanism. Entrainment of sediment particles, therefore, is substantially influenced by bursting events.

Sediment particles move mostly by rolling and sliding with the sweep force and may saltate with higher sweep forces. Thus the impact of the instantaneous sweep force is very important for motion of sediment particles and even more important for the initiation of that motion. Ball and Keshavarzy (1995) pointed out the effect of the instantaneous shear stress on incipient motion and consequent reasons for difficulties in defining sediment entrainment functions. Despite this importance of the bursting events in sediment transport, however, their characteristics have not been investigated in sufficient detail.

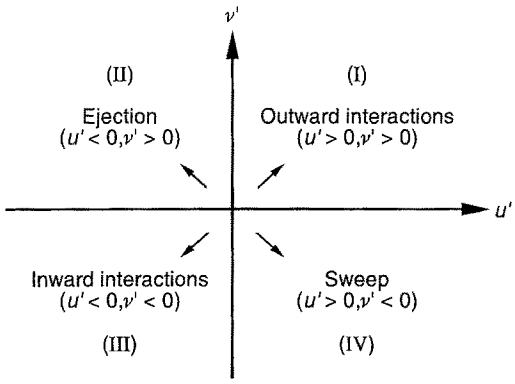

Figure 1. Four classes of bursting event and the associated quadrant.

In the study reported herein the characteristics of the bursting phenomenon in an open channel flow over a rough bed are investigated. The magnitude of the shear stress, the frequency and the angle of events was determined from experimental data. Also determined was the variation of shear stress, frequency and angle for an individual event with respect to depth.

2 Experimental apparatus

The experiments undertaken during this study were carried out in a non-recirculating tilting rectangular flume of 0.61 m width, 0.60 m height and 35 m length. The side walls of the flume were made of glass, making it possible to observe and record the flow. The bed was constructed with movable concrete sheets which are covered by sand particles of 2 mm diameter. As a result, it is possible to perform experiments with different bed roughness simply by changing the concrete sheetS. More detailed descriptions of the experimental flume are presented by Saiedi (1993).

The longitudinal and vertical components of instantaneous velocity were measured using a small electromagnetic velocity meter which will be referred to as an EMC. One advantage of the EMC is that there are no movable parts which can be affected by particles in the water. The EMC probe has two pairs of electrodes and, hence, is able to measure two components of the flow velocity. Use of a trolley mounting device enabled the EMC to be moved to the desired location for the velocity measurement. The measurements were performed in the centerline of the flume at a location of 7 m downstream from the inlet of the flow. An example of the time series of longitudinal and vertical velocity fluctuations obtained during an experiment is shown as Figure 2.

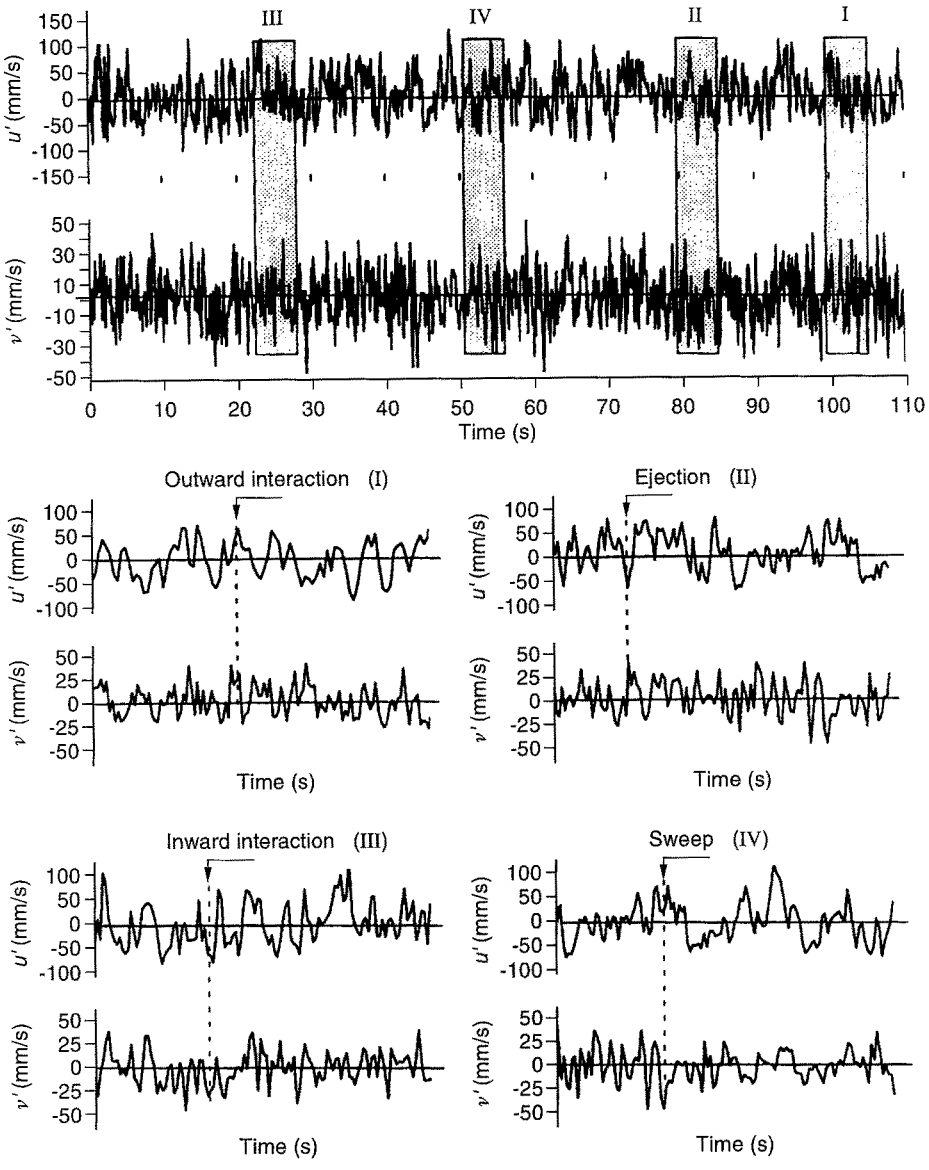

Figure 2. Example of the velocity time series from the experiments.

Velocity components in longitudinal and vertical directions were measured and stored in a digital format for later analysis. This analysis determined the temporal mean velocity in the longitudinal and vertical directions, the temporal mean shear stress, the velocity fluctuations, the mean shear stress for events occurring in each quadrant, and the number of events in each quadrant during the sample period. The analysis also determined the mean angle from the horizontal of events in quadrants II (ejection events) and IV (sweep events).

A summary of the flow parameters for each experiment is shown in Table 1. It was expected that, with these experiments, the effects of the Froude number and the Reynolds number were indirectly considered; the validity of this assumption was assessed by considering non-dimensional velocity profiles determined during the experiments. Shown in Figure 3 are the measured velocity profiles normalized by the cross-section average longitudinal velocity as a function of height above the bed (d) normalized by the flow depth (H); not all the experimental profiles are shown in this figure but those shown are representative of all profiles obtained. The similarity in the non-dimensional velocity profiles shown in Figure 3 validates the assumption of implicit inclusion of the Reynolds and Froude number effects.

3 Analysis of experimental data

Data obtained from the experiments were analyzed to calculate the time-averaged velocity, velocity fluctuations, root mean square, and the Reynolds shear stresses. Relationships used for these calculations were

- The root mean square of the velocity (turbulence intensity)

$$u_{rms} = \sqrt{\overline{u^2}} = \sqrt{\frac{1}{N}\sum_{i=1}^{N}(u_i - \overline{u})^2} \tag{5}$$

and

$$v_{rms} = \sqrt{\overline{v^2}} = \sqrt{\frac{1}{N}\sum_{i=1}^{N}(v_i - \overline{v})^2} \tag{6}$$

- The Reynolds shear stresses were calculated from the velocity fluctuations using

$$\overline{u'v'} = \frac{1}{N}\sum_{i=1}^{N} u_i' v_i' \tag{7}$$

and

$$\tau = -\rho\overline{u'v'} \tag{8}$$

where u_{rms} and v_{rms} are the turbulence intensities in the longitudinal and vertical directions respectively, and τ is the Reynolds shear stress.

Table 1. Hydraulic conditions during experiments

No.	1	2	3	4	5	6	7	8	9	10	11	12
No.	1	2	3	4	5	6	7	8	9	10	11	12
Test	F	G	H	J	K	L	M	N	O	P	Q	
Q(1/s)	63.7	76.3	52	58	73.6	40.2	61	30.3	22	48.5	79.8	97.5
H(mm)	355	154	76	120	145	120	212	154	70	166	230	265
T(degC)	15	15	15	15.5	14	13.5	13.5	13	12.2	13	13	12.6
U(m/s)	0.29	0.81	0.31	0.79	0.83	0.55	0.47	0.32	0.51	0.48	0.57	0.60
U_{max}(m/s)	0.35	0.14	0.38	0.86	0.99	0.65	0.58	0.40	0.56	0.38	0.38	0.37
Fr	0.16	0.66	0.19	0.73	0.7	0.51	0.33	0.26	0.62	0.38	0.38	0.37

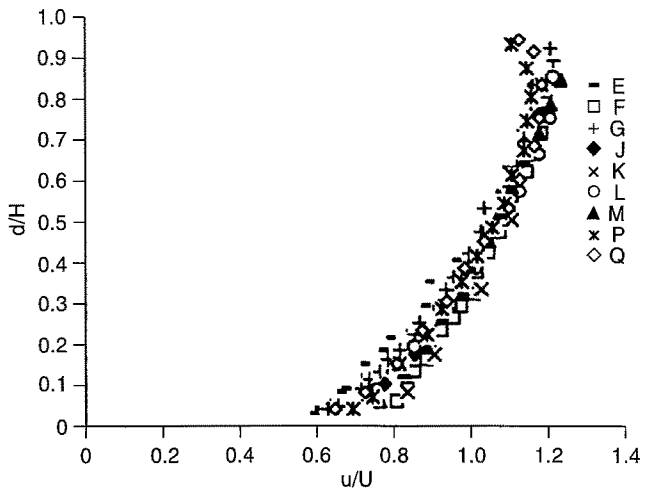

Figure 3. Normalized velocity profiles for experiments

Shown in Figures 4 and 5 are the turbulence intensities normalized by the shear velocity as a function of the measurement height above the channel bed (d) normalized by the flow depth (H). The shear velocity was determined using

$$u_* = \sqrt{\frac{\tau_o}{\rho}} = \sqrt{gRS_f} \tag{9}$$

where u_* is shear velocity, τ_o is shear stress at the bed, R is the hydraulic radius, g is gravitational acceleration and S_f is the friction gradient which, for steady flow conditions, is equal to the energy gradient.

These normalized turbulence intensities were compared with previously published data; as shown in Figures 4 and 5 good agreement between the alternative datasets was obtained. Similar to the previously published data it was found that the turbulence intensity in the longitudinal direction decreased from the bed to the water

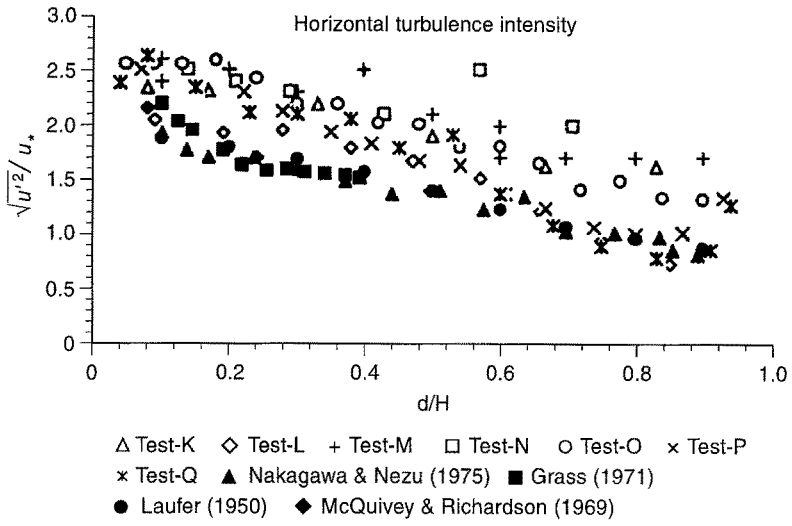

Figure 4. Normalized turbulence intensity in the longitudinal direction.

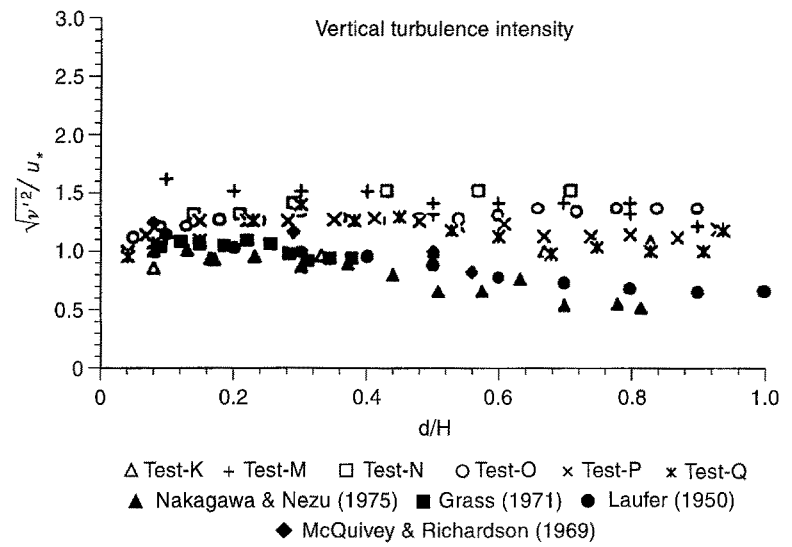

Figure 5. Normalized turbulence intensity in the vertical direction.

surface while the turbulence intensity in the vertical direction was not found to change significantly over the flow depth. In addition, a comparison of normalized Reynolds shear stress with previously published data was undertaken. Shown in Figure 6 are

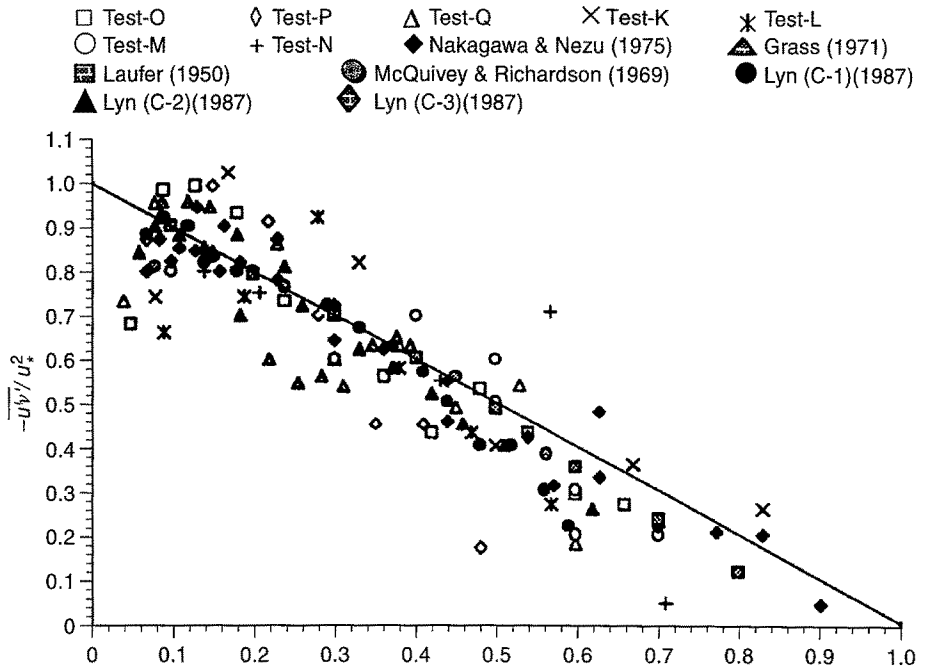

Figure 6. Normalized Reynolds shear stresses.

the nondimensional Reynolds shear stress as a function of the nondimensional vertical location; the data obtained during this study, as indicated in this figure, compares favorably with that previously published.

4 Results and discussion

An analysis of the experimental data indicated that the characteristics of the event classes (sweep, ejection, outward and inward interactions) differed over the flow depth. The following discussion outlines the important aspects obtained from the analysis of the experimental data.

4.1 Instantaneous shear stress of the event classes

The magnitude of the mean shear stress for each quadrant was found to be different, and to differ from the temporal mean shear stress for the flow. The instantaneous shear stress for each event was normalized by the total mean shear stress at that point within the flow. Expressed algebraically, the non-dimensional instantaneous shear stress was determined by

$$C = \frac{\tau}{\overline{\tau}} \tag{10}$$

where τ is the instantaneous shear stress and $\overline{\tau}$ is the mean shear stress at that point in the flow. In order to transform the normalized data into a normally distributed parameter, a Box-Cox power transformation (see Box and Cox, 1964) was used to transform the original data denoted by the symbol C to the transformed data denoted

by B(C). A Box-Cox power transformation is defined, for non-zero values of λ by

$$B(C) = \frac{(C+k)^{\lambda}-1}{\lambda} \tag{11}$$

and, for zero values of λ, by

$$B(C) = \ln(C+k) \tag{12}$$

where k is a constant and λ is transformation power. If all of the values in the time series are greater than zero, then the constant k usually is set to zero (Box and Cox, 1964). Application of the transformation to the data set comprising more tim 50 sets of quadrant IV events (sweep events) and 50 sets of quadrant II events (ejection events) resulted in a value of λ equal to 0.28. Hence, the first case of the transformation (equation 11) is relevant here. The inverse transformation which is the transformation B^{-1} of B(C), for this situation, is given by

$$C = [\lambda B(C)+1]^{\frac{1}{\lambda}} \tag{13}$$

Frequency distributions of the instantaneous shear stresses for events in quadrants IV (sweep) and II (ejection) after application of the transformation are shown in Figure 7. As shown in Figure 8, the transformed data are almost normally distributed. A good normality distribution can be concluded from Figure 8 and consideration of the correlation coefficients of 0.997 and 0.993 obtained for quadrant IV and quadrant II events respectively. As discussed by Looney and Gulledge (1985) and Helsel and Hirsch (1992), the critical correlation coefficients for acceptance of the normality hypothesis with a 0.05 level of significance are 0.993 and 0.991 for events in quadrants IV and II respectively; these values are less than those obtained suggesting that the normality hypothesis can be accepted.

Mean values of the transformed data B(C) for each quadrant were calculated using

$$\left(\overline{B(C)_k} = \frac{1}{n}\sum_{i=1}^{n} B(C_i)\right)_{k=1..4} \tag{14}$$

The inverse Box-Cox transformation was applied to these mean values to enable determination of the mean instantaneous shear stress ratio for events in a particular quadrant. For events in quadrant IV (sweep events), it was found that the magnitude of the shear stress close to the bed of the channel was approximately 150% of the temporal mean shear stress while for events in quadrant II, it was found that the magnitude of the shear stress was approximately 135% of the temporal mean shear stress. Furthermore, as shown in Figures 9 and 10, it was found that the mean shear stress for events in quadrants II and IV increased with depth from the bed to the surface.

Regression equations were developed for the ratio of the mean quadrant shear stress to the temporal mean flow shear stress; these relationships are plotted with 95% confidence limits in Figures 9 and 10. Algebraically, the relationship for quadrant IV events was

$$\overline{C_4} = 1.48 + 1.13\,\frac{d}{H} \tag{15}$$

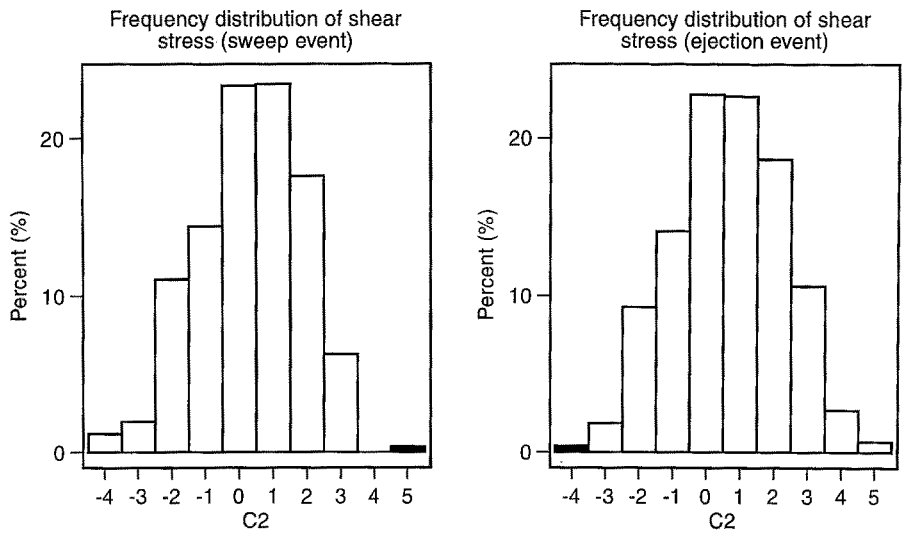

Figure 7. Frequency distributions of transformed data during sweep and ejection events.

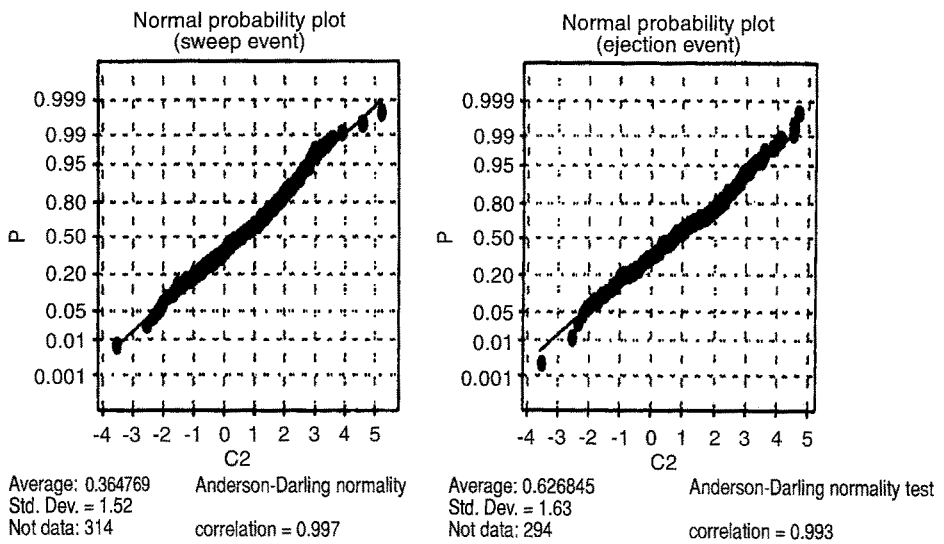

Figure 8. Probability distributions of transformed data during sweep and ejection event.

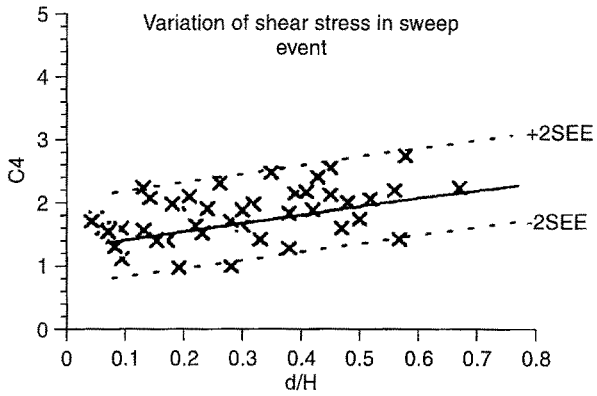

Figure 9. Normalized shear stress in quadrant IV events.

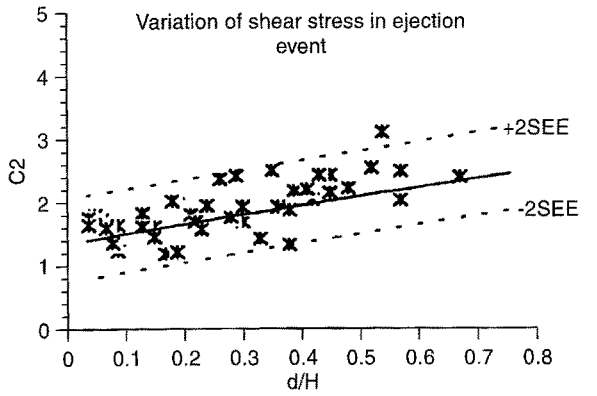

Figure 10. Normalized shear stress in quadrant II events.

and for quadrant II events was

$$\overline{C_2} = 1.35 + 1.83 \frac{d}{H} \tag{16}$$

Correlation coefficients and standard error of estimate for these relationships were 0.73 and 0.36 respectively for quadrant IV events, and 0.81 and 0.38 respectively for quadrant II events.

A focus of this study was the analysis of bursting event characteristics and particularly sweep events in the region close to the channel bed. This focus resulted from a need to consider the influence of the instantaneous shear stress magnitude on the entrainment of sediment particles into the flow. From the analysis described above, the magnitude of the instantaneous shear stress during quadrant IV events on average is approximately 1.40 times the temporal mean shear stress in the region near the channel bed. It is expected, therefore, that particles which would not move at the temporal mean shear stress are able to move during sweep, or quadrant IV, events due to the higher induced shear force. This does not mean, however, that sediment particles are induced into continuous motion but rather are dislodged from their current location.

4.2 Frequency of events

The instantaneous shear stress data was divided into different classes based on the quadrant or phase of the bursting process. The frequency of each quadrant was determined by

$$P_k = \frac{n_k}{N} \tag{17}$$

and

$$N = \sum_{k=1}^{4} n_k \tag{18}$$

where P is the frequency of each event class (quadrant), n_k is the number of occurrences of each event class, N is the total number of events, and the subscript represents the individual quadrants (k =1...4).

The frequency of events in each of the four quadrants was determined from the experimental data and plotted in relation to the normalized depth of flow. Shown in Figures 11 and 12 are the variations in the determined frequency with respect to the normalized depth for each of the four quadrants. It can be seen that the frequency of an individual event varies with the quadrant of the event and the normalized depth. From these figures, it can be seen also that the frequency of events in quadrants IV and II (sweep and ejection events), particularly close to the bed of an open channel, is higher than the frequency of events in quadrants I and III (outward and inward interaction events). Close to the bed, quadrant IV and quadrant II events have a frequency of approximately 30%, whereas that of events in quadrants I and III is approximately 20%. As a result, it can be concluded that sweep and ejection events should occur approximately 30 percent more frequently than outward and inward interaction events.

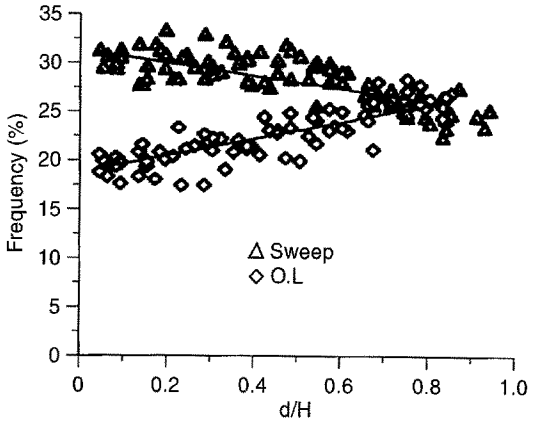

Figure 11. Frequency of events in quadrants IV and I.

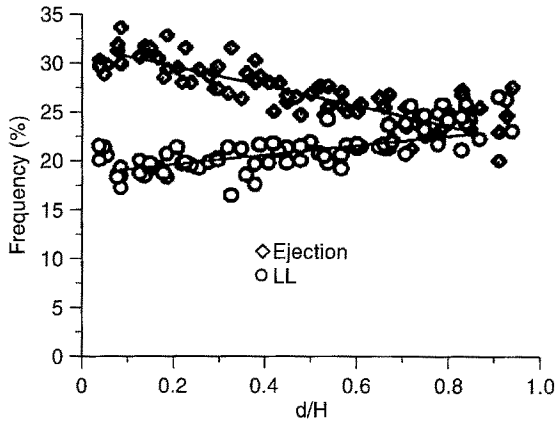

Figure 12. Frequency of events in quadrants II and III.

Additionally, the frequency of the sweep and the ejection events decreases with depth from the bed to the water surface, whereas those of the outward and inward interactions increase with the depth. Furthermore, as shown in Figures 11 and 12, the frequency of all events in all quadrants approaches a value of 25% near the free water surface which suggests that all events are equally probable.

The relationship between the frequency of an event in a quadrant and the normalized depth was investigated with regression relationships developed for estimating the probability of events at a defined normalized depth in quadrants IV and II. The regression relationship for events in quadrant IV (sweep events) was

$$P_4 = \frac{31.9 - (7.2\ \frac{d}{H})}{100} \tag{19}$$

and that for events in quadrant II (ejection events) was

$$P_2 = \frac{31.3 - (8.9\ \frac{d}{H})}{100} \tag{20}$$

Correlation coefficients for these relationships were 0.77 and 0.83 respectively.

4.3 Angle of the events

The force applied to sediment particles on the channel bed during events in quadrant IV depends upon the inclination angle of the force to the bed. The angle of the applied force for individual events was determined from the ratio of the turbulent velocity fluctuations; expressed algebraically, the angle of an event was determined from

$$\theta_k = \arctan\left(\frac{v'}{u'}\right) \tag{21}$$

where θ_k is the angle of the event measured from the horizontal. Similar to the analysis of the shear stress magnitude, it was necessary to apply a Box-Cox transformation to the calculated angles. The mean angle of events in a particular quadrant after application of the transformation was determined then as a function of the normalized depth. The relationships developed for the mean event angle, for events in quadrants IV and II, were

$$\theta_4 = 21.6 + 22.3\ \frac{d}{H} \tag{22}$$

and

$$\theta_2 = 18.8 + 21.2\ \frac{d}{H} \tag{23}$$

respectively. Correlation coefficients for these relationships were 0.67 and 0.71 respectively. Shown in Figures 13 and 14 are the mean angles of the applied force due to events in quadrants IV (sweep) and II (ejection). It can be seen from Figure 13 that the mean angle of events increases with depth from the bed to the free water surface. Close to the bed, the mean angle of sweep events is approximately 20deg-22deg while, near the fixe water surface, the mean angle increases to nearly 45deg. In a similar manner, the mean angle of events in quadrant II is shown in Figure 14 as a function of the normalized depth. Once again, the mean angle of the event increases with the normalized depth; this increase is from approximately 18deg to nearly 45deg at the free water surface.

5 Results and conclusions

The motion of sediment particles and, particularly, the initiation of that motion is an important component of many water quality problems. As the first stage of a study to investigate the entrainment of sediment particles into the flow, the influence of flow turbulence and the associated coherent structures on the shear stress applied to sediment particles was investigated and reported herein. The investigation was based on the analysis of the turbulence characteristics of flows in a laboratory flume with a mobile bed. From the analysis of the experimental data, it was concluded that

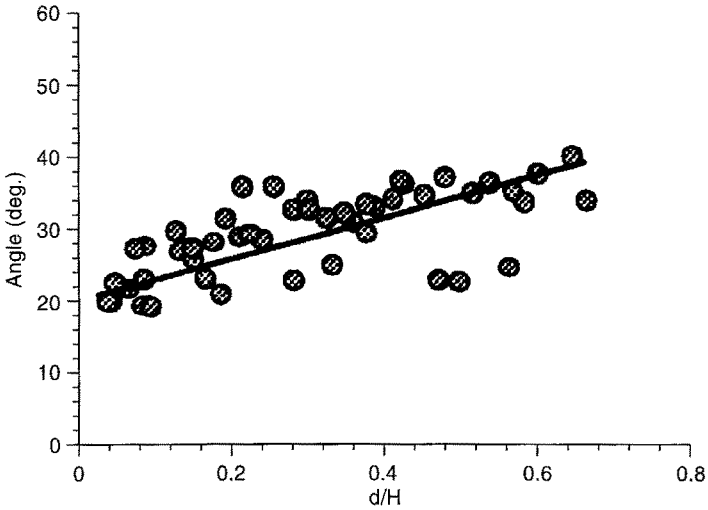

Figure 13. Angle of applied force for events in quadrant IV (sweep events).

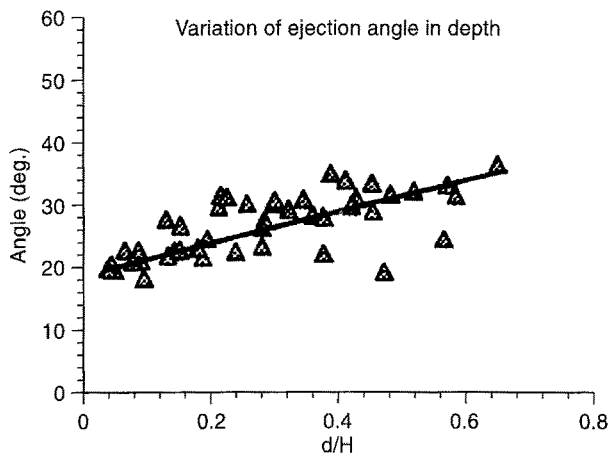

Figure 14. Angle of the applied force for events in quadrant II (ejection events).

- The measured data was consistent with previously published data.
- The magnitude of the mean shear stress in each quadrant (sweep, ejection, outward and inward interactions) was different from the overall temporal mean shear stress at a defined depth within the flow. For quadrant IV events, the mean shear stress was approximately 140% of the overall temporal mean shear stress in the region near the bed and increased to approximately 200% near the free water surface. In quadrant II events, the shear stress ratio is about 1.4 near the bed and increases to approximately 2.5 at the water surface. The shear stress ratios of the quadrant I and III events are low compared to quadrant Iv and II events.
- The frequency of each event was determined also. It was found that, near the bed, the frequency of quadrant IV and II events was approximately 30%, whereas that of quadrant I and III events was only 20%. Consequently, the events in quadrants I and III occur 30% less often than events in quadrants II and IV.
- Also determined was the average angle of action for events in quadrants II and IV. This angle was found to vary with depth from the bed of the channel to the free water surface and to change from approximately 20deg at the bed to 45deg at the water surface for events in quadrant IV. Similar angles for events in quadrant II were found.

The implication of these instantaneous shear stresses is that the instantaneous forces applied to a sediment particles are higher than those suggested through application of Shield's diagram which is based on the overall temporal mean shear stress. Consequently, it is suggested that sediment particles will be induced into motion at lower flow rates than those obtained from Shield's diagram. This motion, however, need not be continuous.

References

Anwar, H.O.; Atkins, R. 1982: Turbulence structure in an open channel flow, Euromech. 156: Mechanics of sediment transport, Istanbul, pp. 19-25

Ball, J.E.; Keshavarzy, A. 1995: Discussion on Incipient Sediment motion on non-horizontal slopes by Chiew and Parker, J. of Hyd. Res. 33(5), 723-724

Bridge, J.S. 1981: Hydraulics interpretation of grain-size distributions using a physical model for bed load transport, J. of Sediment Petrology 51, 1109-1124

Box, G.E.P.; Cox, D.R. 1964: An analysis of transformation, Journal of the Royal Statistical Society, Series B 26, 211-252

Grass, A.J. 1971: Structural features of turbulent flow over smooth and rough boundaries, J. of Fluid Mechanics 50(2), 233-255

Grass, A.J. 1982: The influence of boundary layer turbulence on the mechanics of sediment transport, Euromech 156, Mechanics of sediment transport, Istanbul, pp 3-17

Helsel, D.R.; Hirsch, R.M. 1992: Statistical methods in water resources, Elsevier Science, Amsterdam

Keshavarzy, A.; Ball, J.E. 1995: Instantaneous shear stress on the bed in a turbulent open channel flow, Proc. of XXVI IAHR Congress, London

Kline, S.J.; Reynolds, W.C.; Schraub, F.A.; Runstadler P.W. 1967: The structure of turbulent boundary layers, J. of Fluid Mechanics 30(4), 741-773

Krogstad, P.A.; Antonia, R.A.; Browne, L.W.B. 1992: Comparison between rough and smooth wall turbulent boundary layers, J. of Fluid Mechanics 245, 599-617

Laufer, J. 1950: Some recent measurement in a two dimensional turbulent channel, J. of Aeronautical Science 17(5), 277-287

Looney, S.W.; Gulledge, T.R. 1985: Use of the correlation coefficient with normal probability plots, The American Statistician 39, 75-79

Lyn, D.A. 1986: Turbulence and turbulent transport in sediment-laden open-channel flows, Report No. KH-R-49, W.M. Keck Laboratory of Hydraulics and Water Resources, California Institute of Technology, Pasadena, CA

McQuivey, R.S.; Richardson, E.V. 1969: Some turbulence measurement in open-channel flow, J. of Hydraulics Division, ASCE 95(HY1), 209-223

Nakagawa, H.; Nezu, I.; Ueda H. 1975: Turbulence of open channel flow over smooth and rough beds, Proceeding of the Japan Society of Civil Engineers 241, 155-168

Nakagawa, H.; Nezu, I. 1978: Bursting phenomenon near the wall in open channel flows and its simple mathematical model, Mem. Fac. Eng., Kyoto University, Japan XL(4) 40, 213-240

Nezu, I.; Nakagawa, H. 1993: Turbulence in open-channel flows, IAHR Monograph, Balkema, Rotterdam, The Netherlands

Often, G.R.; Kline, S.J. 1975: A proposed model of the bursting process in turbulent boundary layers, J. of Fluid Mechanics 70(2), 209-228

Raudkivi, A.J. 1990: Loose Boundary Hydraulics, 3rd Ed., Pergamon Press, Oxford

Raupach, M.R. 1981: Conditional statistics of Reynolds stress in rough-wall and smooth-wall turbulent boundary layers, J. of Fluid Mechanics 108, 363-382

Saiedi, S. 1993: Experience in design of a laboratory flume for sediment studies, International Journal of Sediment Research 8(3), 89-101

Thorne, P.D.; Williams, J.J.; Heathershaw, A.D. 1989: In-situ acoustic measurements of marine gravel threshold and transport, Sedimentology 36, 61-74

Williams, J.J. 1990: Video observations of marine gravel transport, Geo. Mar. Lett. 10, 157-164

Yalin, M.S. 1992: River Mechanics, Pergamon Press, Oxford